

## Neutral and cationic Fe(II) $\beta$ -diketiminato complexes

Timo J.J. Sciarone, Auke Meetsma, Bart Hessen \*

*Dutch Polymer Institute/Center for Catalytic Olefin Polymerization, Stratingh Institute for Chemistry and Chemical Engineering,  
University of Groningen, Nijenborgh 4, 9747 AG, Groningen, The Netherlands*

Received 3 June 2005; accepted 29 June 2005

Available online 8 August 2005

Dedicated to Professor Gerard van Koten.

### Abstract

The three-coordinate, 12-valence electron complexes  $[(^{\text{Me}}\text{BDK})\text{FeR}]$  ( $^{\text{Me}}\text{BDK} = [\text{HC}(\text{C}(\text{Me})\text{NAr})_2]^-$ , Ar = 2,6-*i*Pr<sub>2</sub>C<sub>6</sub>H<sub>3</sub>, R = CH<sub>2</sub>Ph, CH<sub>2</sub>SiMe<sub>3</sub>) are reported as well as their reactivity towards Lewis bases. With perfluoroaryl borane and -borate type activators, the monoalkyls react to give alkyl-free paramagnetic cationic iron species counterbalanced by perfluorinated arylborate anions. The paramagnetic nature of the cations permits the observation of weak and dynamic interactions with these anions via <sup>19</sup>F NMR spectroscopy.

© 2005 Elsevier B.V. All rights reserved.

**Keywords:**  $\beta$ -Diketiminato iron(II) complexes; Monoalkyl complexes; X-ray structures; <sup>19</sup>F NMR spectroscopy; Cation–anion interactions

### 1. Introduction

Iron(II) 2,6-diiminopyridine complexes, in conjunction with methyl alumoxane (MAO) cocatalyst, are highly active catalysts for the polymerisation and oligomerisation of ethene [1–5]. Despite this success, little is as yet known about the actual active species in this catalyst system, although an electron-deficient cationic iron(II) monoalkyl species appears to be the most likely candidate. As alkyl abstraction processes from electron-deficient transition-metal alkyl species, and the cation–anion interactions in the resulting ionic products, are basic processes in the generation and action of olefin polymerisation catalysts, we sought to approach this for paramagnetic iron(II) species by studying well-defined electron-deficient iron(II) monoalkyl complexes as model compounds.

$\beta$ -Diketiminato anions of the type  $[\text{HC}\{\text{C}(\text{R})\text{NAr}\}_2]^-$  ( $^{\text{R}}\text{BDK}$ , R = *t*Bu, Me, Ar = 2,6-*i*Pr<sub>2</sub>C<sub>6</sub>H<sub>3</sub>) have found wide employment for stabilisation of low-coordinate complexes of transition metals and main group elements [6]. When coordinating in a chelating fashion to transition metals, they donate 4 electrons while providing steric protection of the metal centre by virtue of the sterically encumbering aryls, which are oriented orthogonal to the planar NCCCN backbone. They seem perfectly suitable for the stabilisation of low coordination number iron(II) alkyl species. Indeed, in recent years, the Holland group [7,8] has reported 12-valence electron, 3-coordinate iron(II) monoalkyls, initially using the 2,5-bis(*tert*-butyl)  $\beta$ -diketiminato ligand  $^{\text{tBu}}\text{BDK}$ . Subsequent efforts by us [9] and the Holland group [10,11] showed that also the smaller ligand  $^{\text{Me}}\text{BDK}$  was capable of stabilising 3-coordinated Fe(II) monoalkyls. Here, we describe the synthesis of the 12-valence electron three-coordinate iron(II) alkyl complexes  $[\text{MeBDK}]\text{FeCH}_2\text{R}$  (R = Ph, SiMe<sub>3</sub>) and alkyl abstraction by Lewis and Brønsted acid activators, together with aspects of the cation–anion interactions in these

\* Corresponding author. Tel.: +31 50 363 4322; fax: +31 50 363 4315.

E-mail addresses: [hessen@chem.rug.nl](mailto:hessen@chem.rug.nl), [B.Hessen@rug.nl](mailto:B.Hessen@rug.nl) (B. Hessen).

ionic species. The paramagnetic nature of the Fe(II) centre is particularly useful in revealing weak cation–anion interactions in solution, as it can effectively act as a chemical shift reagent. A part of this study was communicated previously [9].

## 2. Results and discussion

### 2.1. Synthesis and characterisation of $(^{\text{Me}}\text{BDK})\text{Fe}(\text{II})$ monoalkyl complexes

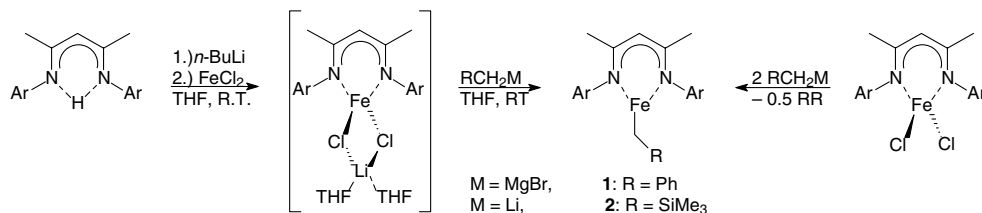
The three-coordinate monoalkyl complexes  $[(^{\text{Me}}\text{BDK})\text{FeR}]$  ( $\text{R} = \text{CH}_2\text{Ph}$ , **1**;  $\text{CH}_2\text{SiMe}_3$ , **2**) were prepared in a one-pot procedure via the ate-complex  $[(^{\text{Me}}\text{BDK})\text{Fe}(\mu\text{-Cl})_2\text{Li}(\text{THF})_2]$  [12] that could be conveniently generated in situ by reaction of  $(^{\text{Me}}\text{BDK})\text{H}$  with  $n\text{-BuLi}$  in THF, followed by reaction with  $\text{FeCl}_2$  or  $\text{FeCl}_2(\text{THF})_{1.5}$ . Subsequent reaction with  $\text{PhCH}_2\text{MgBr}$  or  $\text{LiCH}_2\text{SiMe}_3$  in THF, followed by extraction with and crystallisation from pentane, afforded the alkyl complexes **1** (as red crystals of its pentane solvate) and **2** in 71% and 27% isolated yield, respectively (Scheme 1). The relatively low isolated yield of **2** from this procedure is due to the high solubility of this compound in pentane.

The Fe(II) monoalkyl complexes **1** and **2** are also formed in the reactions of the Fe(III) complex

$[(^{\text{Me}}\text{BDK})\text{FeCl}_2]$  [13] with two equivalents of the respective alkylating agents (Scheme 1). The reaction of  $[(^{\text{Me}}\text{BDK})\text{FeCl}_2]$  with one equivalent of  $\text{PhCH}_2\text{MgBr}$  is accompanied by a colour change from purple to yellow. Addition of the second equivalent of the Grignard reagent induces a colour change to brown-red. The formation of **1** was established by NMR spectroscopy, and GC/MS analysis of the mixture revealed the formation of dibenzyl, *E*-stilbene and toluene. Similar observations were made using  $\text{Me}_3\text{SiCH}_2\text{Li}$  as alkylating agent, and in this case the formation of  $\text{Me}_3\text{SiCH}_2\text{CH}_2\text{SiMe}_3$  and  $\text{SiMe}_4$  as co-products was established. The colour change from purple to yellow upon addition of the first equivalent of alkylating agent indicates that reduction of Fe(III) to Fe(II) takes place in this stage of the reaction. The involvement of free  $\text{RCH}_2\cdot$  radicals in these reductions is suggested by the organic coproducts, which arise from radical dimerisation or hydrogen abstraction processes.

The molecular structures of the  $\beta$ -diketiminato iron monoalkyl complexes **1** and **2** (Fig. 1) were determined by single crystal X-ray diffraction. Pertinent bond lengths and bond angles are listed in Table 1.

Both structures show iron centres coordinated in a trigonal planar fashion, the sum of the angles around iron equalling  $360^\circ$  and  $359^\circ$  for **1** and **2**, respectively. The iron centre is located slightly out of the least-squares



Scheme 1.

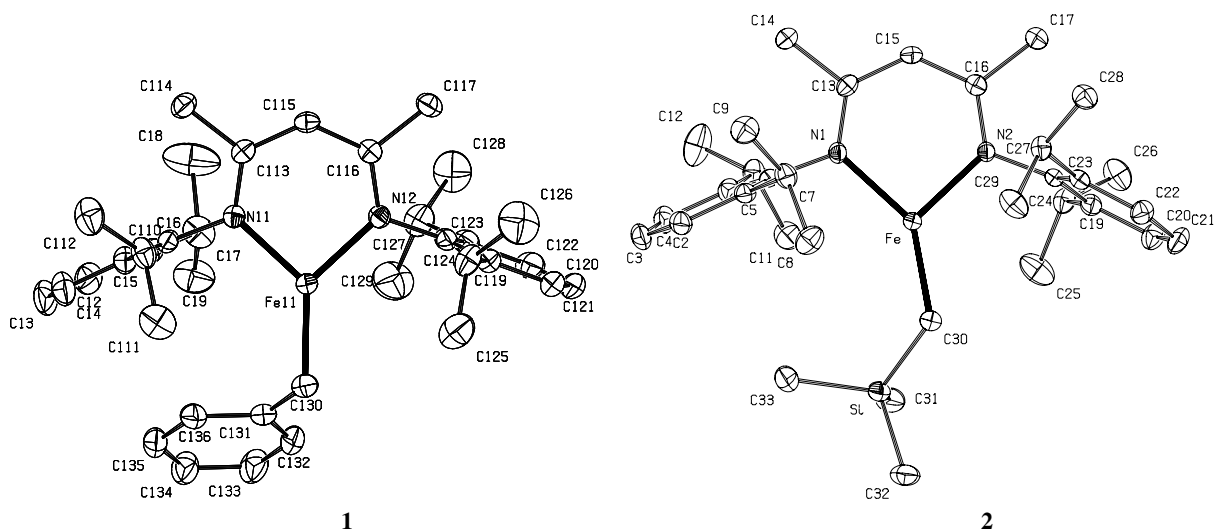


Fig. 1. X-ray structures of **1** and **2** with thermal ellipsoids at 50% probability. Hydrogen atoms have been omitted for clarity.

Table 1  
Selected bond distances and bond angles for **1** and **2**

	<b>1</b>	<b>2</b>
<i>Distances (Å)</i>		
Fe–C30	2.0414(18)	2.0222(18)
Fe–N1	1.9831(11)	1.9915(13)
Fe1–N2	1.9807(11)	1.9926(12)
C13–C15	1.405(2)	1.401(2)
C15–C16	1.401(2)	1.399(2)
N2–C16	1.3405(18)	1.334(2)
N1–C13	1.3321(17)	1.336(2)
<i>Angles (°)</i>		
Fe1–C30–C31	113.18(11)	
Fe–C30–Si		123.48(10)
N1–Fe1–N2	94.35(5)	94.01(5)
C30–Fe–N1	131.81(6)	142.06(6)
C30–Fe–N2	133.84(6)	123.19(6)
C13–C15–C16	128.97(13)	129.14(15)
Fe–N1–C13	124.38(9)	124.34(10)
Fe–N1–C6	115.54(8)	116.67(10)
C6–N1–C13	120.05(11)	118.85(13)
Fe–N2–C16	123.69(10)	125.01(10)
Fe–N2–C18	117.97(9)	114.74(10)
C18–N2–C16	118.32(12)	119.90(12)

plane through the diketiminate NCCCN backbone atoms (0.268(1) Å in **1** and 0.012(1) Å in **2**). The iron–carbon bond lengths (2.0414(18) Å in **1** and 2.0222(18) Å in **2**) lie well in the range of Fe–C distances observed for three-coordinate  $\beta$ -diketiminato iron alkyls [7,8,10,11].

The  $\beta$ -diketiminato ligands coordinate in the normal  $\kappa^2(N,N)$  chelating mode and the aryl substituents on the nitrogen atoms are oriented roughly orthogonal to the coordination plane. The N–Fe–N bite angles of ca. 94° are common for Fe(II)  $\beta$ -diketiminato complexes of [<sup>Me</sup>BDK]<sup>−</sup> [10–14].

Despite the formal electron deficiency of the three-coordinate iron benzyl complex, no interaction between the arene part of the benzyl group and the iron atom is present in **1**. The Fe–C<sub>ipso</sub> distance equals 2.9609(16) Å and Fe–CH<sub>2</sub>–C<sub>ipso</sub> angle = 113.18(11)°, indicating that the aromatic ring of the benzyl group is bent away from the metal. An even larger angle is found in **2** where Fe–CH<sub>2</sub>–Si = 123.48(10)°. The Fe–CH<sub>2</sub>–C<sub>ipso</sub>/Si angles in **1** and **2** are enlarged to minimise steric interactions with the [<sup>Me</sup>BDK]<sup>−</sup> ligand. Steric hindrance of the (trimethylsilyl)methyl group in the small binding pocket of the  $\beta$ -diketiminato ligand is also expressed in the unsymmetric C $\alpha$ –Fe–N angles, which differ by 19° (only 2° difference in **1**). Large differences in the C $\alpha$ –Fe–N angles are also observed in other  $\beta$ -diketiminato Fe(II) monoalkyls with sterically demanding alkyl groups (e.g., [(<sup>Me</sup>BDK)Fe(*i*-Bu)], [(<sup>t</sup>BuBDK)Fe(CH<sub>2</sub>*t*Bu)]) [10,11].

Both the three-coordinate 12 valence electron complexes **1** and **2** are paramagnetic. Both have a magnetic moment in benzene solution of 5.6  $\mu_B$ , consistent with a

high-spin  $d^6$ -configuration (4 unpaired electrons). This is commonly observed in the family of ( $\beta$ -diketiminato)Fe<sup>II</sup>X complexes [7,8,10,11,13,14].

The presence of unpaired electrons in **1** and **2** results in <sup>1</sup>H NMR spectra consisting of paramagnetically shifted, broad resonances in the frequency window from +150 to −150 ppm. The  $\beta$ -diketiminato resonances can be assigned on the basis of integration and comparison to the literature data of related compounds [10,11]. The methylene resonances from the alkyl moieties are not observed, which is consistent with the absence of alkyl  $\alpha$ -CH<sub>2</sub> signals in the spectra of the  $\beta$ -diketiminato iron monoalkyls reported by the Holland group [7,8,10,11].

Solutions and solid samples of **1** and **2** are highly air-sensitive, turning black immediately upon exposure to air. Under inert atmosphere, however, the complexes are thermally very robust. Solutions of **1** or **2** in C<sub>6</sub>D<sub>6</sub> are stable at 80 °C for at least 7 days. In toluene-*d*<sub>8</sub> the monoalkyls are stable as well. No significant decomposition is detected after heating for 8 days at 110 °C. The observed thermostability parallels that of other reported  $\beta$ -diketiminato Fe(II) monoalkyls lacking  $\beta$ -hydrogens [8,10,11,15].

## 2.2. Reactivity toward Lewis bases

Despite their high-spin configuration, with four unpaired electrons, the three-coordinate ( $\beta$ -diketiminato)Fe(alkyl) species still possess one free available valence orbital that should be capable to interact with Lewis basic substrates. Nevertheless, these compounds do not coordinate alkenes, nor show alkene insertion into the Fe–alkyl bond. Thus they are not active as ethene polymerisation catalysts, although single insertion reactions of alkenes into the ( $\beta$ -diketiminato)Fe–hydride bond have been observed [10,11]. With stronger Lewis bases, the alkyl compounds **1** and **2** do show adduct formation. Thus, the benzyl complex **1** forms the adduct [(<sup>Me</sup>BDK)Fe(CH<sub>2</sub>Ph)(py)] (**3**) upon reaction with pyridine. The product crystallises from toluene as deep red crystals of its toluene solvate **3**·(toluene).

A crystal structure determination of **3**·(toluene) (Fig. 2, Table 2) shows a pseudotetrahedral coordination of the iron centre. As expected, the metal–ligand distances are slightly longer than in the three-coordinated parent complex **1**. The Fe–N<sub>py</sub> bond length is considerably longer than the Fe–N<sub>BDK</sub> distances and is comparable to the Fe–N<sup>t</sup>Bupy distance (2.124(2) Å) in the 4-*t*Bu-pyridine adduct of a  $\beta$ -diketiminato Fe(II)-hydride species, [(<sup>t</sup>BuBDK)Fe(H)(4-*t*Bu-py)] [16]. Apart from the slight difference between the two Fe–N<sub>BDK</sub> distances, the geometric parameters relating to the  $\beta$ -diketiminato ligand are unexceptional. The Fe–CH<sub>2</sub>–C<sub>ipso</sub> angle in **3** is ca. 6° larger than in base-free **1**. Again, this is probably the result of increased steric crowding around the metal centre in the four-coordinated complex.

Table 2  
Selected bond distances and bond angles for **3**

Distances (Å)	
Fe–C35	2.107(2)
Fe–N1	2.0253(16)
Fe–N2	2.0393(15)
Fe–N3	2.1154(16)
C13–C15	1.414(3)
C15–C16	1.421(3)
N2–C16	1.340(2)
N1–C13	1.344(2)
Angles (°)	
N1–Fe–N2	92.47(6)
N2–Fe–N3	101.08(6)
N1–Fe–N3	102.78(6)
C35–Fe–N1	126.19(7)
C35–Fe–N2	121.85(7)
C35–Fe–N3	108.54(7)
Fe1–C35–C36	119.18(13)
C13–C15–C16	129.02(17)
Fe–N1–C13	124.97(12)
Fe–N1–C1	114.84(11)
C1–N1–C13	120.14(15)
Fe–N2–C16	124.12(12)
Fe–N2–C18	115.28(11)
C18–N2–C16	120.60(15)

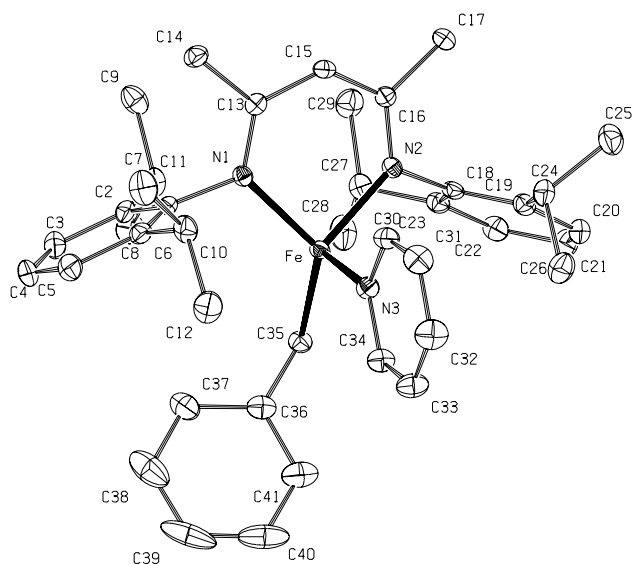
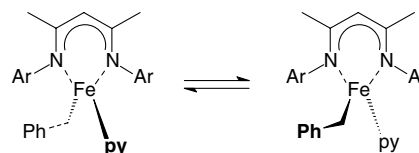


Fig. 2. Molecular structure of **3** with thermal ellipsoids at 50% probability. Hydrogen atoms have been omitted for clarity.

Pyridine adduct **3** possesses a magnetic moment of  $4.4 \mu_B$  in benzene solution, consistent with a high-spin ( $S = 2$ ) Fe(II) centre. The  $^1\text{H}$  NMR spectrum in toluene- $d_8$  at room temperature features extremely broad, overlapping resonances. The line widths and consequent peak overlap are much greater than for the parent compound **1** under similar conditions, suggesting that the molecule shows fluxional behaviour in solution. This process probably involves site-exchange of the coordinated pyridine molecule (Scheme 2). Cooling the solu-



Scheme 2.

tion to  $-50^\circ\text{C}$  reveals 16 sharper resonances. Based on the solid state structure, a maximum of 18 resonances might be expected. The missing resonances may be associated with the protons closest to the paramagnetic centre, the pyridine *ortho* protons and those of the benzyl methylene group. Warming the solution above ambient temperature reveals gradual symmetrisation of the spectrum. At  $110^\circ\text{C}$ , 12 of the maximum 14 resonances expected for a time-averaged  $C_{2v}$ -symmetric molecule are visible in the spectrum. Unfortunately, a full assignment of all the resonances was not possible. The reversibility of the process was confirmed by recooling the sample to room temperature, which restores the original broad spectrum. A related fluxional process was inferred from VT NMR spectroscopy on a few other four-coordinate adduct species  $[(^{\text{Me}}\text{BDK})\text{MX}(\text{L})]$ :  $\text{M} = \text{Fe}$ ,  $\text{X} = \text{NH-2,6-}i\text{Pr}_2\text{C}_6\text{H}_3$ ,  $\text{L} = \text{THF}$ ,  $\text{MeCN}$  [14],  $\text{M} = \text{Ni}$ ,  $\text{X} = \text{Me}$ ,  $\text{L} = 2,4\text{-lutidine}$  [17],  $\text{M} = \text{Mg}$ ,  $\text{Zn}$ ,  $\text{L} = \text{THF}$ ,  $\text{X} = \text{OR}$  [18].

Although the synthesis of **1** and **2**, performed in THF and followed by pentane extraction, affords the base-free 12-electron species, solution NMR spectroscopy suggests that these species also form (relatively weak) Lewis base adducts with THF. Addition of a drop of THF- $d_8$  to a solution of **1** in  $\text{C}_6\text{D}_6$  induces a colour change from red to dark orange. Only 10 signals are observed in the  $^1\text{H}$  NMR spectrum between +70 and  $-100$  ppm (cf. +150 to  $-150$  ppm for **1** in neat  $\text{C}_6\text{D}_6$ ). The number of resonances for  $\mathbf{1} \cdot \text{THF-}d_8$  is consistent with fast site exchange of the THF ligand in the adduct. In neat THF- $d_8$ , site exchange of coordinated solvent in  $\mathbf{1} \cdot \text{THF-}d_8$  is fast on the NMR timescale down to  $-50^\circ\text{C}$ .

### 2.3. Generation of cationic iron $\beta$ -diketiminato complexes

Although the electron-deficient three-coordinate alkyl compounds **1** and **2** are unable to effect catalytic olefin polymerisation, they are interesting model compounds to study the generation of cationic species by alkyl abstraction from the Fe(II) centre through reactions with Lewis or Brønsted acid activators. Reaction of the benzyl complex **1** with the strong Lewis acid  $\text{B}(\text{C}_6\text{F}_5)_3$  in pentane solvent leads to precipitation of the contact ion pair complex  $[(^{\text{Me}}\text{BDK})\text{Fe}\{\eta^2\text{-PhCH}_2\text{B}(\text{C}_6\text{F}_5)_3\}]$  (**4**). The compound was characterised by X-ray diffraction (Fig. 3, Table 3).

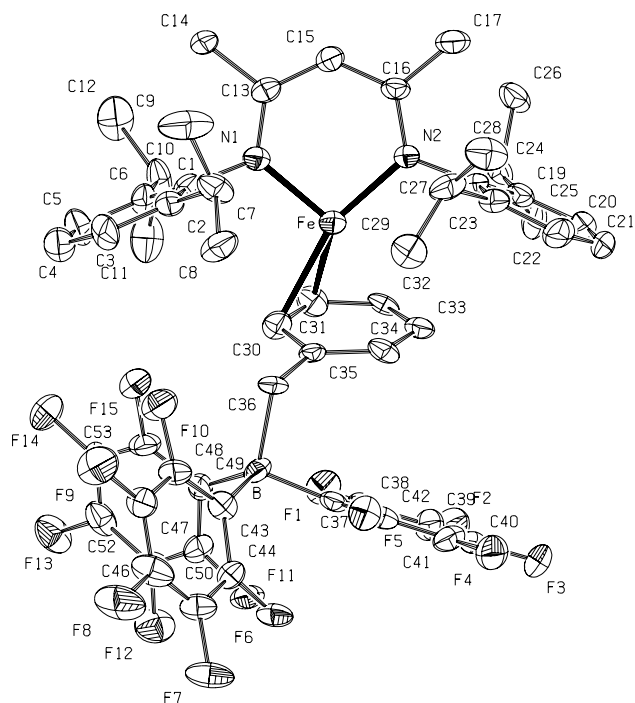


Fig. 3. X-ray structure of **4** with thermal ellipsoids at 50% probability. Hydrogen atoms have been omitted for clarity.

The X-ray structure reveals a contact ion pair in which the benzyl moiety of the  $[\text{PhCH}_2\text{B}(\text{C}_6\text{F}_5)_3]^-$  anion is  $\eta^2$ -coordinated to iron via the *ortho* and *meta* carbon atoms. The description of the coordination mode as (predominantly) dihapto is supported by the distances of the iron centre to C30 and C31, which are at least 0.25 Å shorter than the distances to the other ring carbons. The phenyl C–C bond lengths, however, are identical within experimental error, indicating retention of aromaticity. For the  $[\text{PhCH}_2\text{B}(\text{C}_6\text{F}_5)_3]^-$  anion,  $\eta^3$ - and  $\eta^6$ -interactions of the benzyl fragment with metal centres have been reported previously [19–22]. The  $\eta^2$ -(*m,p*) coordination of this anion as observed in **4** is unprecedented. For the  $[\text{BPh}_4]^-$  anion,  $\eta^2$ -(*m,p*)-coordination to  $[\text{Cp}'_2\text{ZrMe}]^+$  has been proposed based on  $^1\text{H}$  NMR data [23] and  $\eta^2$ -(*o,m*)-coordination of  $[\text{BPh}_4]^-$  to  $[(\text{en})\text{Cu}(\text{CO})]^+$  (*en* = 1,2-diaminoethane) has been established by X-ray diffraction [24].

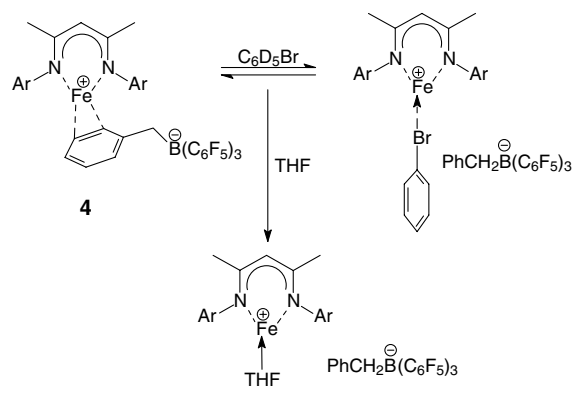
The iron atom is at the centre of a severely distorted tetrahedron comprising the two diketiminato nitrogen atoms and C30 and C31 of the benzyl fragment of the anion. While N1, N2 and C30 are coplanar with iron, C31 is located 1.194(8) Å below this plane. The 2,6-diisopropylphenyl rings make angles of ca. 88° with the coordination plane. The phenyl ring of the coordinated benzyl group and the NCCCNFe-coordination plane are at an angle of 77.1(3)°.

In  $\text{C}_6\text{D}_5\text{Br}$  solution, **4** shows extremely broad and overlapping resonances between –80 and –170 ppm in the  $^{19}\text{F}$  NMR spectrum, suggesting a coordination equi-

Table 3  
Selected bond distances and bond angles for **4**

Distances (Å)	
Fe–N1	1.970(6)
Fe–N2	1.973(6)
Fe–C30	2.344(8)
Fe–C31	2.340(8)
Fe–C32	2.592(7)
Fe–C33	2.741(7)
Fe–C34	2.716(8)
Fe–C35	2.604(7)
C13–C15	1.387(11)
C15–C16	1.401(11)
N2–C16	1.349(8)
N1–C13	1.346(8)
C30–C31	1.383(12)
C31–C32	1.387(13)
C32–C33	1.395(9)
C33–C34	1.400(11)
C34–C35	1.392(12)
C30–C35	1.42(1)
Angles (°)	
N1–Fe–N2	95.9(2)
N1–Fe–C30	103.8(3)
N1–Fe–C31	115.6(3)
N2–Fe–C30	160.3(3)
N2–Fe–C31	134.1(3)
C30–Fe–C31	34.4(3)
Fe–N1–C1	119.2(4)
Fe–N1–C13	122.3(5)
C1–N1–C13	118.5(6)
Fe–N2–C16	123.1(5)
Fe–N2–C18	118.9(4)
C18–N2–C16	117.6(6)
C36–B–C37	103.2(6)
C36–B–C43	111.8(6)
C36–B–C49	113.8(6)
C37–B–C43	113.0(6)
C37–B–C49	112.1(6)
C43–B–C49	103.3(6)
B–C36–C35	114.0(6)

librium between contact ion pair **4** and a solvent-separated ion pair  $[(^{\text{Me}}\text{BDK})\text{Fe}(\text{C}_6\text{D}_5\text{Br})][\text{PhCH}_2\text{B}(\text{C}_6\text{F}_5)_3]$  (Scheme 3).



Scheme 3.

Indeed, variable temperature  $^{19}\text{F}$  NMR spectroscopy demonstrates that at  $-20^\circ$  in  $\text{C}_6\text{D}_5\text{Br}$  solution two perfluorophenyl-containing species are present. The ‘free’

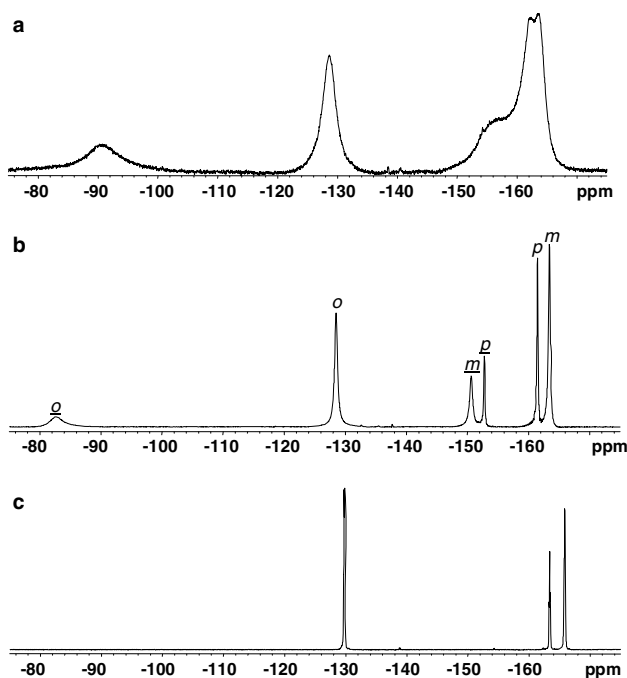
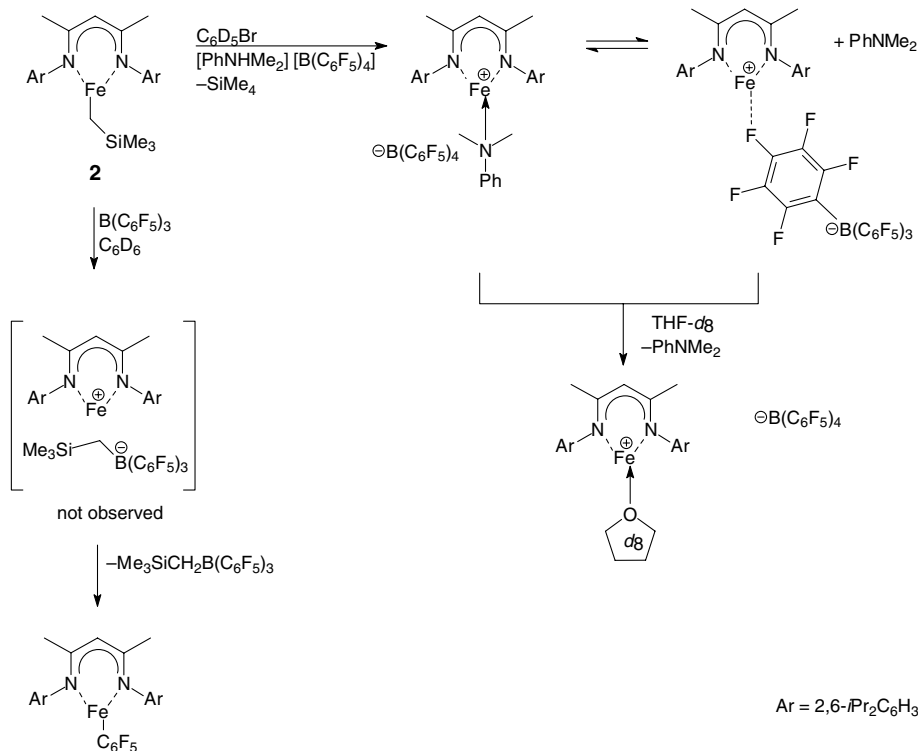


Fig. 4.  $^{19}\text{F}$  NMR spectra of **4** in  $\text{C}_6\text{D}_5\text{Br}$  (188 MHz, ambient temperature) (a), (470 MHz,  $-20^\circ\text{C}$ ) (resonances of contact ion pair are underscored) (b) and **4** +  $\text{THF-}d_8$  (188 MHz, RT) (c).

$[\text{PhCH}_2\text{B}(\text{C}_6\text{F}_5)_3]^-$  anion of the solvent-separated ion pair (71% by integration) shows conventional shifts and sharp  $^{19}\text{F}$  resonances, whereas the bound anion in **4** (29%) is characterised by significant contact shifts and line broadening due to coordination to the paramagnetic Fe(II) centre (Fig. 4). Addition of  $\text{THF-}d_8$  to the sample affords the corresponding adduct  $[(^{\text{Me}}\text{BDK})\text{Fe}(\text{THF-}d_8)][\text{PhCH}_2\text{B}(\text{C}_6\text{F}_5)_3]$ , yielding the  $^{19}\text{F}$  NMR spectrum of the unperturbed  $[\text{PhCH}_2\text{B}(\text{C}_6\text{F}_5)_3]^-$  anion.

Abstraction of the (trimethylsilyl)methyl group from  $[(^{\text{Me}}\text{BDK})\text{FeCH}_2\text{SiMe}_3]$  (**2**) was investigated by NMR tube scale experiments. An orange solution of **2** in  $\text{C}_6\text{D}_6$  turns dark yellow immediately after addition of the Lewis acid  $\text{B}(\text{C}_6\text{F}_5)_3$  and changes to bright red in the course of 1 h. At that stage, the  $^{19}\text{F}$  NMR spectrum exhibits three sharp signals characteristic of the borane  $\text{Me}_3\text{SiCH}_2\text{B}(\text{C}_6\text{F}_5)_2$  [25,26]. In addition, two broad resonances are observed at  $\delta = +118.1$  ( $\Delta\nu_{1/2} = 64$  Hz) and  $+31.5$  ( $\Delta\nu_{1/2} = 345$  Hz) ppm, with an integral ratio of 1:2. These shifts suggest that  $\text{C}_6\text{F}_5$  transfer to the metal has occurred to give  $[(^{\text{Me}}\text{BDK})\text{Fe}(\text{C}_6\text{F}_5)]$  (Scheme 4). The *ortho* fluorine resonances of the Fe– $\text{C}_6\text{F}_5$  species are not detected, possibly due to extreme line broadening by the paramagnetic centre. The  $^1\text{H}$  NMR spectrum shows paramagnetic ligand resonances of a single  $\text{C}_{2v}$ -symmetric  $\beta$ -diketiminato-supported Fe(II) compound, which is consistent with the formulation of  $[(^{\text{Me}}\text{BDK})\text{Fe}(\text{C}_6\text{F}_5)]$ .

Transfer of a pentafluorophenyl group from  $\text{B}(\text{C}_6\text{F}_5)_3$  to Fe(II) was recently reported by Chirik [27] in the reac-



Scheme 4.

tion of  $[(\alpha\text{-diimine})\text{Fe}(\text{CH}_2\text{SiMe}_3)_2]$  with  $\text{B}(\text{C}_6\text{F}_5)_3$ , yielding  $\text{Me}_3\text{SiCH}_2\text{B}(\text{C}_6\text{F}_5)_2$  and  $[(\alpha\text{-diimine})\text{Fe}(\text{CH}_2\text{SiMe}_3)(\text{C}_6\text{F}_5)]$ . Although the spectroscopic data reported for the borane are identical to those observed by us, the  $^{19}\text{F}$  NMR shifts attributed by the authors to the paramagnetic  $\text{Fe}-\text{C}_6\text{F}_5$  complex ( $\delta = -162.3, -154.0, -139.1$  ppm) appear in a region very different from those in our case, and essentially lie in the normal diamagnetic chemical shift range.

The reaction of **2** with the Brønsted acid  $[\text{PhNHMe}_2][\text{B}(\text{C}_6\text{F}_5)_4]$  in  $\text{C}_6\text{D}_5\text{Br}$  solvent was used to generate the cation  $[(^{\text{Me}}\text{BDK})\text{Fe}]^+$  with the perfluorinated borate counterion  $[\text{B}(\text{C}_6\text{F}_5)_4]^-$ . The reaction was accompanied by liberation of  $\text{SiMe}_4$  and a colour change from yellow to purple-red. No resonances for free *N,N*-dimethylaniline could be observed in the spectrum, but a very broad resonance at  $\delta = 30.8$  ppm ( $\Delta\nu_{1/2} = 1596$  Hz), integrating as 3H, was seen in addition to resonances attributable to the  $^{\text{Me}}\text{BDK}$  ligand of the paramagnetic iron species. This suggests coordination of the aniline to the paramagnetic metal centre (Scheme 4). The broad resonance observed may be associated with the aniline protons farthest removed from the metal centre (phenyl *p*-H and *m*-H). Despite the apparent coordination of the aniline, the  $^{19}\text{F}$  NMR spectrum also gives indication of some degree of association of the  $[\text{B}(\text{C}_6\text{F}_5)_4]^-$  anion with the paramagnetic centre: its resonances are significantly shifted relative to the normal positions of the free anion (Fig. 5(a)). This indicates that the aniline and the anion are in dynamic equilibrium with respect to their interaction with the metal centre. Indeed, upon addition of an aliquot of THF-*d*<sub>8</sub> a colour change from purple-red to green is seen and the  $^{19}\text{F}$  NMR spectrum now showed resonances normal for the free anion (Fig. 5(b)). Consistently, the  $^1\text{H}$  NMR

spectrum now shows free *N,N*-dimethylaniline ( $\delta = 2.69$  ppm, 6H,  $\text{PhNMe}_2$ ) and formation of a single  $\text{C}_{2v}$ -symmetric paramagnetic compound, presumably the THF-*d*<sub>8</sub>-adduct  $[(^{\text{Me}}\text{BDK})\text{Fe}(\text{THF-}d_8)]^+$ . Very recently, Gregory et al. reported the cationic  $\beta$ -diketiminate Fe(II) complex  $[(^{\text{tBu}}\text{BDK})\text{Fe}(\text{Et}_2\text{O})]^+$ , which was prepared from the monomethyl derivative and  $[\text{Ph}_3\text{C}][\text{B}\{3,5-(\text{CF}_3)_2\text{C}_6\text{H}_3\}_4]$  in diethyl ether solution [28].

### 3. Conclusions

The three-coordinate Fe(II) monoalkyl complexes  $[(^{\text{Me}}\text{BDK})\text{FeR}]$  ( $\text{R} = \text{CH}_2\text{Ph}$ , **1**;  $\text{CH}_2\text{SiMe}_3$ , **2**) were readily synthesised in a one-pot procedure. Although these 12 valence electron  $S = 2$  species do not coordinate or polymerise alkenes, they do interact with Lewis bases to form pseudo-tetrahedral adducts. For pyridine this interaction is strong enough to allow isolation of the adduct, but the weaker base THF readily dissociates from the metal centre upon work-up.

The two alkyl complexes can be used as model systems to study the generation of ionic species by alkyl abstraction reactions and the interactions between the cation and anion in these species, features that are of general relevance to the generation and action of cationic olefin polymerisation catalysts. The paramagnetic nature of the cationic species allows it to act as a chemical shift reagent, revealing weak and dynamic cation–anion interactions with fluorinated arylborate anions by  $^{19}\text{F}$  NMR spectroscopy. This was possible even for the very weakly nucleophilic  $[\text{B}(\text{C}_6\text{F}_5)_4]^-$  anion, suggesting that the application of paramagnetic metal centres may be of more general use in the study of weak cation–anion interactions in solution.

### 4. Experimental

#### 4.1. General considerations and instrumentation

All iron complexes are highly air-sensitive and were handled under a dry dinitrogen atmosphere using standard Schlenk and drybox techniques. Diethyl ether and THF (99.9% Aldrich) were percolated over a column of  $\text{Al}_2\text{O}_3$  and stored under nitrogen. Toluene, hexanes and pentane (99.9% Aldrich) were percolated over a column packed with molecular sieves 4 Å (90 wt%) and  $\text{Al}_2\text{O}_3$  (10 wt%) and stored under nitrogen. Deuterated solvents ( $\text{C}_6\text{D}_6$ , THF-*d*<sub>8</sub> Aldrich) were dried over Na/K alloy and stored under nitrogen.  $\text{C}_6\text{D}_5\text{Br}$  (Aldrich) was distilled from  $\text{CaH}_2$ .

NMR-spectra were recorded on Varian Inova 500, VXR 300 and Varian Gemini 200 instruments.  $^1\text{H}$  chemical shifts are referenced to residual protons in

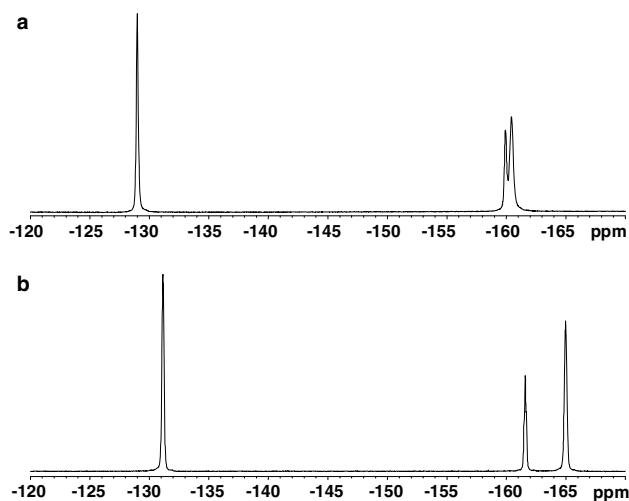


Fig. 5.  $^{19}\text{F}$  NMR (188 MHz, ambient temperature) spectra of **2** +  $[\text{PhNHMe}_2][\text{B}(\text{C}_6\text{F}_5)_4]$  before (a) and after (b) addition of an aliquot of THF-*d*<sub>8</sub>.

deuterated solvents and are reported relative to tetramethylsilane.  $^1\text{H}$  NMR spectra of paramagnetic compounds were recorded with pulse widths of ca.  $25^\circ$  and acquisition times of ca. 200 ms using a window wide enough to place no peaks near the edge of the spectrum. If possible, concentrations of ca. 50 mg/0.5 mL were used. IR-spectra were recorded on a Mattson 4020 Galaxy FT-IR spectrometer. GC-MS analyses were conducted using a HP 5973 mass-selective detector attached to a HP 6890 GC instrument. Elemental analyses were performed by the Microanalytical Department at the University of Groningen or by Mikroanalytisches Laboratorium H. Kolbe, Mülheim an der Ruhr, Germany. Reported values are the averages of two independent determinations. Effective magnetic moments (calculated as  $\mu_{\text{eff.}} = 2.828\sqrt{\chi_{\text{m}}T}$ ) were determined by Evans' method in  $\text{C}_6\text{H}_6$  at RT [29,30]. The data are corrected for diamagnetism using Pascal's constants [31].

#### 4.2. Starting materials

$[\text{Me}^c\text{BDK}]\text{H}$  [32],  $\text{LiCH}_2\text{SiMe}_3$  [33],  $\text{FeCl}_2$  [34],  $\text{FeCl}_2(\text{THF})_{1.5}$  [35], and  $\text{B}(\text{C}_6\text{F}_5)_3$  [36] were prepared by the literature procedures.  $[(\text{BDK})\text{FeCl}_2]$  was prepared according to a modification of a published procedure [13] using THF as reaction solvent and diethyl ether for extraction and crystallisation.  $\text{FeCl}_3$  (Acros), acetylacetonone, 2,6-diisopropylaniline,  $[\text{Ph}_3\text{C}][\text{B}(\text{C}_6\text{F}_5)_4]$  (Strem) and  $[\text{PhNHMe}_2][\text{B}(\text{C}_6\text{F}_5)_4]$  (Asahi Glass Co.) were commercial products and were used without further purification.

#### 4.3. Preparation of $[(\text{Me}^c\text{BDK})\text{FeCH}_2\text{Ph}] \cdot 0.5\text{C}_5\text{H}_{12}$ (**1**) $\cdot 0.5\text{C}_5\text{H}_{12}$

*n*-BuLi (2.5 M in hexanes) (3.8 mL, 9.6 mmol) was added to a stirred solution of  $[\text{Me}^c\text{BDK}]\text{H}$  (4.0 g, 9.6 mmol) in THF (30 mL). The solution was stirred for 30 min at room temperature.  $\text{FeCl}_2$  (1.21 g, 9.6 mmol) was added and the resulting yellow suspension was stirred for 18 h.  $\text{PhCH}_2\text{MgBr}$  (1.43 M in  $\text{Et}_2\text{O}$ ) (6.7 mL, 9.6 mmol) was added. The solution turned red immediately and was stirred for 4 h at room temperature. THF was evaporated under reduced pressure. Residual THF was removed by suspending the dark residue in pentane (30 mL, 3 $\times$ ) followed by removal of pentane in vacuo. The residue was extracted with pentane (100 mL, 4 $\times$ ). The extract was filtered, concentrated to ca. 75% and stored at  $-25^\circ\text{C}$  for 48 h to give red crystals. Yield: 4.1 g (71%).

$^1\text{H}$  NMR (500 MHz,  $\text{C}_6\text{D}_6$ , RT):  $\delta$  ( $\Delta\nu_{1/2}$ , integral, assignment) = 117.2 (787 Hz, 1H,  $\alpha$ -H), 56.4 (349 Hz, 6H,  $\gamma$ -Me), 45.1 (115 Hz, H, *m*- $\text{H}_{\text{Bz}}$ ), 40.4 (1238 Hz, 2H, *o*- $\text{H}_{\text{Bz}}$ ),  $-8.7$  (55 Hz, 4H, *m*- $\text{H}_{\text{Ar}}$ ),  $-17.6$  (102 Hz, 12H, *iPr*-Me),  $-43.6$  (60 Hz, 1H, *p*- $\text{H}_{\text{Bz}}$ ),  $-75.8$

(77 Hz, 2H, *p*- $\text{H}_{\text{Ar}}$ ),  $-112.3$  (651 Hz, 12H, *iPr*-Me),  $-119.4$  (1302 Hz, 4H, *iPr*-CH) ppm.

$\mu_{\text{eff.}}(\text{C}_6\text{H}_6, 298\text{ K}) = 5.6 \mu_{\text{B}}$ .

Anal. Calc. for  $\text{C}_{36}\text{H}_{48}\text{N}_2\text{Fe} \cdot 0.5\text{C}_5\text{H}_{12}$  (600.71) requires: C, 76.98; H, 9.06; N, 4.66; Fe, 9.30. Found: C, 77.47; H, 9.31; N, 4.74; Fe, 9.00%.

#### 4.4. Reaction of **1** with THF- $d_8$

A few drops of THF- $d_8$  (excess) were added to a solution of **1** (20 mg, 33  $\mu\text{mol}$ ) in  $\text{C}_6\text{D}_6$  (0.5 mL). The colour of the solution changed from red to dark orange.

$^1\text{H}$  NMR (500 MHz,  $\text{C}_6\text{D}_6$ , RT):  $\delta$  ( $\Delta\nu_{1/2}$  integral, assignment) = 68.0 (667 Hz, 1H,  $\alpha$ -H), 42.3 (95 Hz, 2H, *m*- $\text{H}_{\text{Bz}}$ ), 20.3 (1071 Hz, 2H, *o*- $\text{H}_{\text{Bz}}$ ), 18.0 (323 Hz, 6H,  $\gamma$ -Me),  $-1.6$  (47 Hz, 4H, *m*- $\text{H}_{\text{Ar}}$ ),  $-11.2$  (89 Hz, 12H, *iPr*-Me),  $-45.5$  (51 Hz, 1H, *p*- $\text{H}_{\text{Bz}}$ ),  $-64.8$  (64 Hz, 2H, *p*- $\text{H}_{\text{Ar}}$ ),  $-82.7$  (515 Hz, 12H, *iPr*-Me),  $-93.0$  (1547 Hz, 4H, *iPr*-CH) ppm.

#### 4.5. Preparation of $[(\text{Me}^c\text{BDK})\text{FeCH}_2\text{SiMe}_3]$ (**2**)

*n*-BuLi (2.5 M in hexanes, 1.67 mL, 4.18 mmol) was added to a stirred solution of the  $\beta$ -diketimine (1.75 g, 4.18 mmol) in THF (20 mL). The pale yellow solution was stirred for 30 min.  $\text{FeCl}_2(\text{THF})_{1.5}$  (982 mg, 4.28 mmol) was added as a solid. The resulting yellow solution was stirred for 45 min.  $\text{LiCH}_2\text{SiMe}_3$  (394 mg, 4.18 mmol) was added as a solid and a very dark solution was obtained. After 30 min the solution had become dark red. After another 15 min stirring, all THF was removed under reduced pressure. Any residual THF was removed by stirring the residue with pentane (25 mL) and subsequent evaporation of all volatiles (3 $\times$ ). Next, the residue was extracted with pentane (30 mL, 2 $\times$ ). The orange extract was concentrated to ca. 10 mL and cooled to  $-25^\circ\text{C}$  to afford **2** as yellow crystals. Yield: 624 mg (27%). The yield was not optimised.

$^1\text{H}$  NMR (500 MHz,  $\text{C}_6\text{D}_6$ , RT):  $\delta$  ( $\Delta\nu_{1/2}$ , integral, assignment) = 115.5 (720 Hz, 1H,  $\alpha$ -CH), 74.7 (350 Hz, 6H,  $\gamma$ - $\text{CH}_3$ ), 56.1 (396 Hz, 9H,  $\text{Si}(\text{CH}_3)_3$ ),  $-9.0$  (50 Hz, 4H, *m*-H),  $-14.5$  (101 Hz, 12H, *iPr*- $\text{CH}_3$ ),  $-68.5$  (65 Hz, 2H, *p*-H),  $-100.4$  (530 Hz, 12H, *iPr*- $\text{CH}_3$ ),  $-126.9$  (1766 Hz, 4H, *iPr*-CH) ppm.

$\mu_{\text{eff.}}(\text{C}_6\text{H}_6, 298\text{ K}) = 5.6 \mu_{\text{B}}$ .

Anal. Calc. for  $\text{C}_{33}\text{H}_{52}\text{N}_2\text{FeSi}$  (560.72) requires: C, 70.69; H, 9.35; N, 5.00. Found: C, 70.82; H, 9.26; N, 5.06%.

#### 4.6. Reaction of **2** with $\text{B}(\text{C}_6\text{F}_5)_3$

Alkyl complex **2** (25 mg, 45  $\mu\text{mol}$ ) was dissolved in  $\text{C}_6\text{D}_6$  (0.5 mL). To this solution was added  $\text{B}(\text{C}_6\text{F}_5)_3$  (23 mg, 45  $\mu\text{mol}$ ). The orange solution turned slightly darker. Complete conversion was reached in the course of 2 days at RT, giving a bright red solution.

$[(^{Me}BDK)Fe(C_6F_5)]$ :  $^1H$  NMR (500 MHz,  $C_6D_6$ , RT)  $\delta$  ( $\Delta\nu_{1/2}$ ) = 96.1 (486 Hz, 1H,  $\alpha$ -H), 70.2 (242 Hz, 6H,  $\gamma$ -CH<sub>3</sub>), 7.3 (11.7 Hz, 4H, *m*-ArH), -9.7 (79.9 Hz, 12H, *iPr*-CH<sub>3</sub>), -71.0 (67.4 Hz, 1H, *p*-ArH), -84.7 (298 Hz, 12H, *iPr*-CH<sub>3</sub>), -139.0 (1219 Hz, 4H, *iPr*-CH) ppm.

$^{19}F$  NMR (188 MHz,  $C_6D_6$ , RT)  $\delta$  = 118.1 (s, br,  $\Delta\nu_{1/2}$  = 63.7 Hz, 1F, *p*-F), 31.5 (s, br,  $\Delta\nu_{1/2}$  = 345.0 Hz, 2F, *m*-F).

$Me_3SiCH_2B(C_6F_5)_2$ :  $^1H$  NMR (500 MHz,  $C_6D_6$ , RT)  $\delta$  = 2.16 (s, 2H,  $CH_2SiMe_3$ ), 0.07 (s, 9H,  $CH_2SiMe_3$ ) ppm.

$^{19}F$  NMR (188 MHz,  $C_6D_6$ , RT)  $\delta$  = -130.9 (d,  $J_{FF}$  = 20 Hz, 2F, *o*-F), -148.6 (t,  $J_{FF}$  = 20 Hz, 1F, *p*-F), -162.2 (m, 2F, *m*-F) ppm.

#### 4.7. Reaction of **2** with $[PhNHMe_2][B(C_6F_5)_4]$ and reaction with THF- $d_8$

$[PhNHMe_2][B(C_6F_5)_4]$  (36 mg, 44.6  $\mu$ mol) was added to a solution of **2** (25 mg, 44.6  $\mu$ mol) in  $C_6D_5Br$  (0.5 mL). A dark purple/red solution was obtained.

$^{19}F$  NMR (188 MHz,  $C_6D_5Br$ , RT):  $\delta$  = -129.0 (30 Hz, 2F, *o*-F), -159.9 (34 Hz, 1F, *p*-F), -160.4 (58 Hz, 2F, *m*-F) ppm.

$^1H$  NMR (400 MHz,  $C_6D_5Br$ , RT)  $\delta$  = 54.2 (187, 6H,  $\gamma$ -Me), 50.7 (357, 1H,  $\alpha$ -H), 30.8 (1596, 3H, *m,p*-H<sub>Ph</sub> of  $PhNMe_2$ ), 8.8 (35, 4H, *m*-H<sub>Ar</sub>), -5.1 (75, 12H, *iPr*-CH<sub>3</sub>), -76.1 (63, 2H, *p*-H<sub>Ar</sub>), -77.3 (253, 12H, *iPr*-CH<sub>3</sub>), -111 (954, 4H, *iPr*-CH) ppm. No resonances were observed for the *N*-Me and *o*-H<sub>Ph</sub> protons of the coordinated *N,N*-dimethylaniline molecule.

A drop of THF- $d_8$  was added to the NMR tube. A colour change from dark purple/red to bright green was observed.

$^{19}F$  NMR (188 MHz,  $C_6D_5Br$ , RT):  $\delta$  = -131.1 (38 Hz, 2F, *o*-F), -161.6 (44 Hz, 1F, *p*-F), -165.0 (47 Hz, 2F, *m*-F) ppm.

$^1H$  NMR (400 MHz,  $C_6D_5Br$ , RT)  $\delta$  = 21.9 (34, 4H, *m*-H<sub>Ar</sub>), 7.7 (79, 12H, *iPr*-CH<sub>3</sub>), -8.8 (145, 12H, *iPr*-CH<sub>3</sub>), -39.3 (38, 2H, *p*-H<sub>Ar</sub>), -60.0 (131, 6H,  $\gamma$ -Me), -95.1 (329, 1H,  $\alpha$ -H) ppm. No resonance for the *iPr*-CH protons was observed, possibly due to extreme line broadening. Formation of free *N,N*-dimethylaniline was noted ( $\delta$  = 2.69 ppm, 6H,  $PhNMe_2$ ).

#### 4.8. Preparation of $[(^{Me}BDK)Fe(CH_2Ph)(py)]$ (**3**)

Benzyl complex **1** (200 mg, 0.35 mmol) was dissolved in toluene (5 mL). Pyridine (1 mL, 12 mmol) was allowed to diffuse into the solution. Dark red crystals of composition  $[(^{Me}BDK)Fe(CH_2Ph)(py)] \cdot$  toluene had formed after 16 h. The crystals (69 mg) were isolated by filtration and dried in vacuo. A second crop (75 mg) of spectroscopically identical crystals was obtained by concentration of the filtrate. Combined yield: 144 mg (0.20 mmol, 57%).

$^1H$  NMR (500 MHz,  $PhMe-d_8$ , -50 °C): ( $\Delta\nu_{1/2}$ , integral, assignment) = 58.2 (107 Hz, 1H,  $\alpha$ -H), 50.9 (249 Hz, 2H, *m*-H<sub>Ph</sub>), 48.1 (329 Hz, 1H, *m*-H<sub>py</sub>), 33.6 (292 Hz, 1H, *m*-H<sub>py</sub>), 27.5 (130 Hz, 2H, *m*-H<sub>Ar</sub>), 21.1 (143 Hz, 2H, *m*-H<sub>Ar</sub>), 14.6 (312 Hz, 6H, *iPr*-CH<sub>3</sub>), -2.8 (137 Hz, 6H, *iPr*-CH<sub>3</sub>), -8.9 (427 Hz, 6H, *iPr*-CH<sub>3</sub>), -18.6 (693 Hz, 6H, *iPr*-CH<sub>3</sub>), -24.7 (1784 Hz, 1H, *o*-H<sub>py</sub>), -41.3 (2345 Hz, 1H, *o*-H<sub>py</sub>), -60.3 (146 Hz, 2H, *p*-H<sub>Ar</sub>), -76.2 (149 Hz, 1H, *p*-H<sub>Ph</sub>), -103.1 (594 Hz, 1H, *p*-H<sub>py</sub>), -125.7 (478 Hz, 6H,  $\gamma$ -CH<sub>3</sub>) ppm.

$\mu_{eff.}(C_6H_6, 298 K) = 4.4 \mu_B$ .

*Anal.* Calc. for  $C_{41}H_{53}N_3Fe$  (643.74) requires: C, 76.50; H, 8.30; N, 6.53. Found: C, 76.68; H, 8.35; N, 6.42%. Although  $^1H$  NMR spectroscopy in  $C_6D_6$  showed the presence of toluene in the crystals, elemental analysis was satisfactory for the solvent-free complex, suggesting loss of toluene from the crystal lattice.

#### 4.9. Preparation of $[(^{Me}BDK)Fe\{\eta^2-PhCH_2B(C_6F_5)_3\}]$ (**4**)

A solution of  $B(C_6F_5)_3$  (426 mg, 0.83 mmol) in pentane (20 mL) was added slowly to a stirred solution of **1** (500 mg, 0.83 mmol) in pentane (30 mL). The red solution almost instantaneously turned dark and a precipitate was formed. The precipitate was filtered off and repeatedly washed with pentane (50 mL, 8 $\times$ ). The brown powder was dried in vacuo. Yield: 598 mg, 67% based on **1**.

*Anal.* Calc. for  $C_{54}H_{48}N_2FeBF_{15}$  (1076.62) requires: C, 60.24; H, 4.49; N, 2.60. Found: C, 59.62; H, 4.29; N, 2.60%.

$^1H$  NMR (300 MHz, THF- $d_8$  RT):  $\delta$  ( $\Delta\nu_{1/2}$ ) = 21.3 (26), 11.7 (10), 7.0 (71), 6.6 (17), 6.5 (33), 6.3 (18), 4.4 (6), 3.5 (31), 3.2 (7), 2.7 (13), 2.4 (30), 1.4 (18), 1.2 (9), 0.8 (25), 0.7 (19), 0.6 (19), 0.4 (23) -8.7 (134), -17.7 (117), -25.2 (149), -37.2 (26) -38.5 (49), -39.7 (30), -52.0 (94), -55.9 (97), -60.2 (138), -94.6 (299) ppm.

$^{19}F$  NMR (188 MHz, THF- $d_8$  RT):  $\delta$  = -131.8 (d,  $J_{FF}$  = 21 Hz, 6F, *o*-F), -167.3 (t,  $J_{FF}$  = 20 Hz, 3F, *p*-F), -169.5 (m, 6F, *m*-F).

$^{19}F$  NMR (188 MHz,  $C_6D_5Br$ , RT):  $\delta$  = -89.7 (br), -167.3 (br), -169.5 (br, with shoulder -157.7).

$^{19}F$  NMR (470 MHz,  $C_6D_5Br$ ) variable temperature spectra were recorded from -20 to +30 °C with 5 °C intervals using 20 mg of **4** dissolved in 0.5 mL solvent.

$^1H$  NMR (500 MHz,  $C_6D_5Br$ , -20 °C):  $\delta$  ( $\Delta\nu_{1/2}$ ) = 68.3 (457), 47.2 (698), 23.7 (67), 22.4 (429), 9.1 (278), 8.2 (294), 7.2 (18), 6.9 (13), 6.9 (17), 4.8 (26), 3.4 (45), 2.8 (29), 1.6 (20), 1.1 (30), 1.0 (49), 0.8 (71), 0.7 (26), -0.5 (122), -3.9 (187), -9.2 (9374), -11.7 (273), -48.8 (120), -68.2 (166), -73.4 (288), -76.2 (362) ppm.

$^{19}F$  NMR (470 MHz,  $C_6D_5Br$ , -20 °C):  $\delta$  = -82.6 (*o*-F), -128.4 (*o*-F), -150.7 (*m*-F), -152.8 (*p*-F), -161.5 (*p*-F), -163.4 (*m*-F) ppm.

#### 4.10. Reaction of **4** with THF-*d*<sub>8</sub>

To a solution of **4** (20 mg) in C<sub>6</sub>D<sub>5</sub>Br (0.5 mL) was added a drop of THF-*d*<sub>8</sub>. The dark brown solution turned bright yellow instantaneously.

<sup>19</sup>F NMR (188 MHz, C<sub>6</sub>D<sub>5</sub>Br, RT):  $\delta = -129.7$  (d,  $J_{\text{FF}} = 20.3$  Hz, 6F, *o*-F),  $-163.3$  (t,  $J_{\text{FF}} = 19.2$  Hz, 3F, *p*-F),  $-165.8$  (m, 6F, *m*-F) ppm.

#### 4.11. Crystal structure determinations

Crystals were mounted on top of a glass fiber, by using inert-atmosphere handling techniques, and aligned on a Bruker SMART APEX CCD diffractometer ( $\lambda$  (Mo K $\alpha$ ) = 0.71073 Å) [37]. Intensity data were corrected for Lorentz and polarization effects, scale variation, for decay and absorption: a multi-scan absorption correction was applied, based on the intensities of symmetry-related reflections measured at different angular settings (SADABS), and reduced to  $F_o^2$  [38]. The program suite SHELXTL was used for space group determination (XPREP) [39].

##### 4.11.1. Crystal refinement details for **1**

Suitable crystals were obtained by recrystallisation from pentane. From the solution it was clear that both pentane solvent molecules were located over an inversion centre, implying disorder. A disorder model with a s.o.f. of 0.5 for both pentanes was used in the refinement. No classic hydrogen bonds, no missed symmetry (*MISSYM*) or solvent-accessible voids were detected by procedures implemented in PLATON [40,41].

C<sub>23</sub>H<sub>48</sub>N<sub>2</sub>Fe · C<sub>5</sub>H<sub>12</sub>,  $M = 1201.37$ , red platelet crystal, 0.45 × 0.40 × 0.12 mm, space group  $P2_1/c$ , #14 [42],  $a = 15.3319(9)$ ,  $b = 20.652(1)$ ,  $c = 22.408(1)$  Å,  $\beta = 90.781(1)^\circ$ ,  $V = 7094.5(6)$  Å<sup>3</sup>,  $Z = 4$ ,  $\mu = 4.52$  cm<sup>-1</sup>, 44924 reflections collected at 125(1) K, 18149 unique reflections ( $R_{\text{int}} = 0.276$ ), 13810 reflections observed with [ $F_o \geq 4.0(F_o)$ ], 1181 refined parameters,  $R(F)$  for  $F_o \geq 4\sigma(F_o) = 0.0430$ ,  $wR(F^2) = 0.1134$ , max. residual electron density  $-0.24$  and  $0.52(6)$  e Å<sup>-3</sup>.

##### 4.11.2. Crystal refinement details for **2**

Suitable crystals were obtained by recrystallisation from pentane. No classic hydrogen bonds, no missed symmetry (*MISSYM*), but potential solvent-accessible area (voids of 29.2 Å<sup>3</sup>/unit cell) were detected by procedures implemented in PLATON [40,41].

C<sub>33</sub>H<sub>52</sub>N<sub>2</sub>FeSi,  $M = 560.72$ , orange, block crystal, 0.28 × 0.21 × 0.12 mm, space group  $P2_1/n$ , #14 [42],  $a = 10.5957(5)$ ,  $b = 21.292(1)$ ,  $c = 14.7768(7)$  Å,  $\beta = 97.218(1)^\circ$ ,  $V = 3307.3(3)$  Å<sup>3</sup>,  $Z = 4$ ,  $\mu = 5.14$  cm<sup>-1</sup>, 30277 reflections collected at 100(1) K, 8215 unique reflections ( $R_{\text{int}} = 0.0414$ ), 6349 reflections observed with [ $F_o \geq 4.0\sigma(F_o)$ ], 539 refined parameters,  $R(F)$  for

$F_o \geq 4\sigma(F_o) = 0.0392$ ,  $wR(F^2) = 0.0997$ , max. residual electron density  $-0.22$  and  $0.43(6)$  e Å<sup>-3</sup>.

##### 4.11.3. Crystal refinement details for **3**

Suitable crystals were obtained by crystallisation from toluene. No classic hydrogen bonds, no missed symmetry (*MISSYM*) or solvent-accessible voids were detected by procedures implemented in PLATON [40,41].

C<sub>41</sub>H<sub>53</sub>N<sub>3</sub>Fe · C<sub>7</sub>H<sub>8</sub>,  $M = 735.88$ , red, platelet crystal, 0.45 × 0.38 × 0.065 mm, space group  $P-1$ , #2 [42],  $a = 9.2518(8)$ ,  $b = 12.091(1)$ ,  $c = 19.640(2)$  Å,  $\beta = 82.446(1)^\circ$ ,  $V = 2152.5(3)$  Å<sup>3</sup>,  $Z = 2$ ,  $\mu = 3.85$  cm<sup>-1</sup>, 17162 reflections collected at 100(1) K, 8581 unique reflections ( $R_{\text{int}} = 0.0354$ ), 6748 reflections observed with [ $F_o \geq 4.0\sigma(F_o)$ ], 713 refined parameters,  $R(F)$  for  $F_o \geq 4\sigma(F_o) = 0.0414$ ,  $wR(F^2) = 0.0985$ , max. residual electron density  $-0.27$  and  $0.34(5)$  e Å<sup>-3</sup>.

##### 4.11.4. Crystal refinement details for **4**

Suitable crystals were obtained by recrystallisation from bromobenzene. No classic hydrogen bonds, no missed symmetry (*MISSYM*), but potential solvent-accessible area (voids of 71.0 Å<sup>3</sup>/unit cell) were detected by procedures implemented in PLATON [40,41].

C<sub>54</sub>H<sub>48</sub>N<sub>2</sub>FeBF<sub>15</sub>,  $M = 1076.62$ , red, platelet crystal, 0.15 × 0.14 × 0.08 mm, space group  $C2/c$ , #15 [42],  $a = 44.806(3)$ ,  $b = 13.349(1)$ ,  $c = 17.780(1)$  Å,  $\beta = 113.282(5)^\circ$ ,  $V = 9768.5(12)$  Å<sup>3</sup>,  $Z = 8$ ,  $\mu = 4.060$  cm<sup>-1</sup>, 34522 reflections collected at 110(1) K, 11209 unique reflections ( $R_{\text{int}} = 0.3431$ ), 3022 reflections observed with [ $F_o \geq 4.0\sigma(F_o)$ ], 851 refined parameters,  $R(F)$  for  $F_o \geq \sigma(F_o) = 0.0678$ ,  $wR(F^2) = 0.1767$ , max. residual electron density  $-0.51$  and  $0.43(8)$  e Å<sup>-3</sup>.

#### Acknowledgement

This research was financially supported by the Dutch Polymer Institute (project #106).

#### Appendix A. Supplementary data

CIF files have been deposited with the Cambridge Crystallographic Data Centre, CCDC Nos. 185601 (**1**), 273724 (**2**), 273725 (**3**), and 185603 (**4**). Copies of these data may be obtained free of charge on application to The Director, CCDC, 12 Union Road, Cambridge CB2 1EZ, UK, fax: +44 1223 336 033, email: deposit@ccdc.cam.ac.uk or on the web www: <http://www.cam.ac.uk>. IR spectral data of the isolated compounds, additional NMR data and experimental details are available from the author upon request. Supplementary data associated with this article can be found, in the online version, at doi:10.1016/j.ica.2005.06.065.

## References

- [1] B.L. Small, M. Brookhart, A.M.A. Bennett, *J. Am. Chem. Soc.* 120 (1998) 4049.
- [2] B.L. Small, M. Brookhart, *J. Am. Chem. Soc.* 120 (1998) 7143.
- [3] G.J.P. Britovsek, V.C. Gibson, B.S. Kimberley, P.J. Maddox, S.J. McTavish, G.A. Solan, A.J.P. White, D.J. Williams, *Chem. Commun.* (1998) 849.
- [4] G.J.P. Britovsek, M. Bruce, V.C. Gibson, B.S. Kimberley, P.J. Maddox, S. Mastroianni, S.J. McTavish, C. Redshaw, G.A. Solan, S. Stromberg, A.J.P. White, D.J. Williams, *J. Am. Chem. Soc.* 121 (1999) 8728.
- [5] G.J.P. Britovsek, S. Mastroianni, G.A. Solan, S.P.D. Baugh, C. Redshaw, V.C. Gibson, A.J.P. White, D.J. Williams, M.R.J. Elsegood, *Chem. – Eur. J.* 6 (2000) 2221.
- [6] L. Bourget-Merle, M.F. Lappert, J.R. Severn, *Chem. Rev.* 102 (2002) 3031.
- [7] H. Andres, E.L. Bominaar, J.M. Smith, N.A. Eckert, P.L. Holland, E. Münck, *J. Am. Chem. Soc.* 124 (2002) 3012.
- [8] J.M. Smith, R.J. Lachicotte, P.L. Holland, *Organometallics* 21 (2002) 4808.
- [9] T.J.J. Sciarone, A. Meetsma, B. Hessen, J.H. Teuben, *Chem. Commun.* (2002) 1580.
- [10] J. Vela, J.M. Smith, R.J. Lachicotte, P.L. Holland, *Chem. Commun.* (2002) 2886.
- [11] J. Vela, S. Vaddadi, T.R. Cundari, J.M. Smith, E.A. Gregory, R.J. Lachicotte, C.J. Flaschenriem, P.L. Holland, *Organometallics* 23 (2004) 5226.
- [12] J.M. Smith, R.J. Lachicotte, P.L. Holland, *Chem. Commun.* (2001) 1542.
- [13] A. Panda, M. Stender, R.J. Wright, M.M. Olmstead, P. Klavins, P.P. Power, *Inorg. Chem.* 41 (2002) 3909.
- [14] N.A. Eckert, J.M. Smith, R.J. Lachicotte, P.L. Holland, *Inorg. Chem.* 43 (2004) 3306.
- [15] P.L. Holland, T.R. Cundari, L.L. Perez, N.A. Eckert, R.J. Lachicotte, *J. Am. Chem. Soc.* 124 (2002) 14416.
- [16] J.M. Smith, R.J. Lachicotte, P.L. Holland, *J. Am. Chem. Soc.* 125 (2003) 15752.
- [17] H.L. Wiencko, E. Kogut, T.H. Warren, *Inorg. Chim. Acta* 345 (2003) 199.
- [18] M.H. Chisholm, J.C. Huffman, K. Phomphrai, *J. Chem. Soc., Dalton Trans.* (2001) 222.
- [19] C. Pellecchia, A. Immirzi, A. Grassi, A. Zambelli, *Organometallics* 12 (1993) 4473.
- [20] M. Bochmann, S.J. Lancaster, M.B. Hursthouse, K.M.A. Malik, *Organometallics* 13 (1994) 2235.
- [21] C. Pellecchia, A. Grassi, A. Immirzi, *J. Am. Chem. Soc.* 115 (1993) 1160.
- [22] L.W.M. Lee, W.E. Piers, M.R.J. Elsegood, W. Clegg, M. Parvez, *Organometallics* 18 (1999) 2947.
- [23] A.D. Horton, J.H.G. Frijns, *Angew. Chem., Int. Ed. Engl.* 30 (1991) 1152.
- [24] M. Pasquali, C. Floriani, A. Gaetani-Manfredotti, *Inorg. Chem.* 19 (1980) 1191.
- [25] P. Chirik, Personal communication (16-3-2004).
- [26] R.E.v.H. Spence, W.E. Piers, Y. Sun, M. Parvez, L.R. MacGillivray, M.J. Zaworotko, *Organometallics* 17 (1998) 2459.
- [27] S.C. Bart, E.J. Hawrelak, A.K. Schmisser, E. Lobkovsky, P.J. Chirik, *Organometallics* 23 (2004) 237.
- [28] E.A. Gregory, R.J. Lachicotte, P.L. Holland, *Organometallics* 24 (2005) 1803.
- [29] E.M. Schubert, *J. Chem. Educ.* 69 (1992) 62.
- [30] D.F. Evans, *J. Chem. Soc.* (1959) 2003.
- [31] O. Kahn, *Molecular Magnetism*, VCH, New York, 1993.
- [32] P.H.M. Budzelaar, N.N.P. Moonen, R. de Gelder, J.M.M. Smits, A.W. Gal, *Eur. J. Inorg. Chem.* (2000) 753.
- [33] H.L. Lewis, T.L. Brown, *J. Am. Chem. Soc.* 92 (1970) 4664.
- [34] P. Kovacic, N.O. Brace, *Inorg. Synth.* 6 (1960) 172.
- [35] R.J. Kern, *J. Inorg. Nucl. Chem.* 24 (1962) 1105.
- [36] J.L.W. Pohlmann, F.E. Brinckmann, *Z. Naturforsch.* 20b (1965) 5.
- [37] SMART, SAINT, SADABS, XPREP and SHELXTL/NT, Area Detector Control and Integration Software, Smart Apex Software Reference Manuals, Bruker Analytical X-ray Instruments. Inc., Madison, WI, USA, 2000.
- [38] G.M. Sheldrick, SADABS – V2 – Multi-Scan Absorption Correction Program, University of Göttingen, Göttingen, Germany, 2001.
- [39] G.M. Sheldrick, SHELXL-97 – Program for the Refinement of Crystal Structures, University of Göttingen, Göttingen, Germany, 2003.
- [40] A.L. Spek, PLATON – Program for the Automated Analysis of Molecular Geometry (A Multipurpose Crystallographic Tool), University of Utrecht, Utrecht, The Netherlands, 2002.
- [41] A.L. Spek, *Acta Crystallogr., Sect. A* 46 (1990) C34.
- [42] International Tables for Crystallography, Kluwer Academic Publishers, Dordrecht, The Netherlands, 1992.